Positive expression of ZNF689 indicates poor prognosis of hepatocellular carcinoma

PENG SHENG YI, BIN WU, DA WEI DENG, GUANG NIAN ZHANG and JIAN SHUI LI

Department of Hepato-Biliary-Pancrease, Institute of General Surgery,
The Affiliated Hospital of North Sichuan Medical College, Nanchong, Sichuan 639000, P.R. China

Received November 26, 2017; Accepted June 1, 2018

DOI: 10.3892/ol.2018.9295

Abstract. The objective of the present study was to investigate the association between zinc finger protein (ZNF) 689 expression and the clinicopathological features and prognosis of hepatocellular carcinoma (HCC). A total of 102 paired HCC and paired non-cancerous tissues, and 16 normal liver tissues were collected. ZNF689 expression was examined in HCC tissues, paired-noncancerous tissues, and normal liver tissues using RT-qPCR and immunohistochemistry analysis, and the association between ZNF689 expression and HCC prognosis was analyzed using the Kaplan-Meier method. ZNF689 expression was not significantly different between HCC tissues and paired-noncancerous tissues (P=0.61). ZNF689 expression in HCC and paired-noncancerous tissues was significantly increased compared with that in normal liver tissues (P<0.01). Positive expression of ZNF689 protein in HCC was significantly associated with a tumor size of ≥10 cm, tumor capsule infiltration, and microvascular invasion (P<0.05). Positive expression of ZNF689 was a prognostic factor for overall survival time [hazard ratio (HR):1.961; P=0.048] and progression-free survival time (HR:1.902; P=0.041). ZNF689 maybe a novel predictor for prognosis of patients with HCC.

Introduction

Hepatocellular carcinoma (HCC) is one of the most common cancer types globally, and the fifth highest cause of cancer-associated mortality (1). The etiology of HCC differs between regions; hepatitis C infection and alcohol abuse are the most common causes of HCC in western countries, while in China the majority of patients with HCC harbor a hepatitis B (HBV) infection (2,3). A variety of treatments are recommended for HCC, with radical treatments including radical resection, liver transplantation and radiofrequency ablation being recommended for the treatment of early stage HCC. Patients diagnosed with advanced stage HCC are candidates for palliative treatments, including sorafenib and other targeted treatments (4,5). In total, ~30% of all patients with HCC are diagnosed at an advanced stage in China (6), and novel treatments are required in orderto improve the prognosis of these patients.

Zinc finger proteins (ZNF) are a family of DNA binding proteins, encoded by 2% of all human genes (7). Generally, ZNFs are divided into eight categories: C2H2 like (Cys2His2), Gag knuckle, treble clef, zinc ribbon, Zn2/Cys6, TAZ2 domain like, Zinc binding loops and metallothionein (8). C2H2 type zinc finger protein is the largest of these groups. Previous studies have revealed an association between ZNF expression and HCC prognosis; Wang *et al* (9) demonstrated that increased zinc finger and BTB domain containing 20 (ZBTB20) expression is associated with poor HCC prognosis, and Kan *et al* (10) recently reported that ZBTB20 is an independent prognostic biomarker for HCC. Yang *et al* (11) analyzed 92 HCC tumor tissue samples and identified that zinc finger E-box binding homeo box 2 expression was associated with tumor metastasis. Recently, Wu *et al* (12) determined that ZNF191 inhibited HCC metastasis by inactivating discs large 1-mediated yes-associated protein.

ZNF689, a C2H2 type ZNF, is a putative transcription regulating factor. A previous study demonstrated that the knockdown of ZNF689 results in tumor cell growth inhibition (8). It has also been identified that ZNF689 inhibited tumor cell apoptosis via downregulation of the pro-apoptotic factors B cell lymphoma (Bcl)2 antagonist/killer 1, Bcl2 associated X protein (Bax) and BH3 interacting domain death agonist (Bid) (13). In the aforementioned study, immunohistochemical analysis was also performed on HCC tumor samples and it was revealed that 4/12 cases presented with nuclear expression of ZNF689. In order to further explore whether ZNF689 is a novel treatment target and its significance in determining HCC prognosis, the present study used an increased number of specimens to analyze the association between ZNF689 expression and the baseline characteristics of patients with HCC.

Materials and methods

Patients and follow-up. A total of 102 paired HCC tissues and adjacent non-cancerous tissues were collected from patients

Correspondence to: Professor Jian Shui Li, Department of Hepato-Biliary-Pancrease, Institute of General Surgery, The Affiliated Hospital of North Sichuan Medical College, 63 Wenhua Road, Nanchong, Sichuan 639000, P.R. China
E-mail: 15208207079@163.com

Key words: zinc finger protein 689, hepatocellular carcinoma, prognosis, clinicopathological feature

who underwent radical liver resection between January 2011 and December 2012 in West China Hospital of Sichuan University (Chengdu, Sichuan Province, China), including 93 males and 9 females. Patients who were diagnosed by histological detection and with a preserved liver function (Child A,B), without prior systematic therapy or local treatments prior to liver resection were included; additionally patients who withdrew from follow-up or without sufficient clinical data were excluded. Written informed consent was obtained from all enrolled patients, and the study was ethically approved by the Biomedical Ethics Committee of West China Hospital. The median patient age was 55 years (range, 21-76), with 42 patients ≥60 years (41.2%). A total of 51 patients (50%) presented with an α-fetoprotein level >400 ng/ml, and 96 patients (94.1%) presented with positive expression of the HBV surface antigen. Among all patients, tumor size ranged from 1.5 to 13.8 cm (median size, 6.0 cm). Tumor differentiation was classified as high differentiation, moderate differentiation or low differentiation (14). According to the Barcelona Clinical Liver Cancer system (BCLC), HCC was classified as early stage (BCLC A), intermediate stage (BCLC B), or advanced stage (BCLC C) (4). A total of 15 patients (14.7%) were staged as BCLC A, 48 (47.1%) as BCLC B, and 39 (38.2%) as BCLC C. Liver function was measured by Child-Pugh grade system, which is the most common evaluating system for liver function. It comprises five variables total bilirubin, prothrombin time, albumin, ascites, and hepatic encephalopathy. Child A is defined as score 5,6, Child B is defined as score 7-9 (15). No patients received radiofrequency ablation or trans-arterial chemoembolization prior to liver resection. Liver tissues were collected <15 min after liver resection and stored at -80˚C. Paired non-cancerous tissue was defined as liver tissue >3 cm from the tumor resection edge. All frozen liver samples tested in the present study were stored in the Clinical Sample Bank of West China Hospital. Follow-up was performed at one to three-month intervals via an outpatient visit or telephone call. Recurrence was defined as new lesions within the residual liver or distant organ metastasis detected by ultrasound, computed tomography or magnetic resonance imaging scans. Follow-up was completed in May 2016.

Reverse transcription-quantitative polymerase chain reaction (RT-qPCR). Total RNA was extracted from each specimen using TRIzol® reagent (Life Technologies; Thermo Fisher Scientific, Inc., Waltham, MA, USA) according to the manufacturer's protocol. RNA concentration was determined with a ScanDrop Nuclear Acid Analyzer (AnalytikJenaAG, Jena, Germany). To determine the integrity of RNA, 3 μg of each RNA sample was separated on a 1% denatured agarose gel and then detected via a Chemical Mpimaging system (Bio-Rad, Laboratories, Inc, Hercules, CA, USA). If the peak area of the 28S ribosome RNA (rRNA) was approximately twice that of 18S rRNA, the integrity of the total RNA was considered as acceptable and used for continued investigation. ZNF689 mRNA was quantified using RT-qPCR, with primers designed via Primer 5.0 software (PremierBiosoft, International, Palo Alto, CA, USA), and synthesized by Sangon Biotech (Shanghai, China) (Table I). The reference gene used for qPCR is GAPDH, the detail sequence was listed in Table I. cDNA was synthesized using a RevertAid First-Strand cDNA Synthesis kit (ThermoFisher Scientific, Inc.), and qPCR was performed in triplicate for each sample using Maxima SYBR Green qPCR Master mix (Thermo Fisher Scientific, Inc.) on the CFX connect Real-Time system (Bio-Rad, Laboratories, Inc.). Amplification proceeded for 3 min at 95˚C for denaturing, followed by 40 cycles for ZNF689 and GAPDH, at 95˚C for 15 sec, 60˚C for 30 sec in the CFX connect Real-Time system. Relative expression levels of each gene were calculated using the $2^{-\Delta\Delta Cq}$ method (16).

Cell culture and transfection. The normal hepatic cell line LO2 and HCC cell lines (Huh7, MHCC97H, and Hep3B) were purchased from the Cell Bank of Type Culture Collection of the Chinese Academy of Sciences (Shanghai, China). HCC cell lines were preserved in Dulbecco's modified Eagle's medium (DMEM) (Hyclone, GE Healthcare Life Sciences, Logan, UT, USA). LO2 cells were maintained in RPMI-1640 medium (Invitrogen; Thermo Fisher Scientific, Inc.) supplemented with 10% fetal bovine serum (FBS) (Hyclone; GE Healthcare Life Sciences), 100 units/ml penicillin, and 100 mg/ml streptomycin. Cells were placed in a humidified atmosphere containing 5% CO_2 at 37˚C. Cells were transfected with lentivirus or plasmids using Turbo transfection reagent. Lentivirus were purchased from Shanghai Genechem Co Ltd (Shanghai, China) shRNA were loaded by GV208, EGFP, and AMP vectors. Trans-KD™ Easy was used as transfection reagent, and purchased from Shanghai Genechem Co Ltd. Transfection incubation was set at 37˚C for 48 h.

HCC cell migration and wound-healing assays. To perform a transwell migration assay, $1x10^5$ cells obtained from MHCC-97 shRNA transfection (M-Si) cell line were seeded into the upper chamber of transwell plates (BD Biosciences, Franklin Lakes, NJ, USA) with serum-free DMEM. The lower chamber was filled with DMEM containing 10% FBS. After incubation for 48 h at 37˚C, cells in the upper surface of the filters were softly removed by a cotton swap, then cells migrating to the lower surface of the filters were fixed inethanol for 20 min at room temperature. Cells were randomly counted in eight fields, from threedifferent membranes. Considering Wound-healing assay, Cells in logarithmic growth phase were cultured in a 6-well plate until 90% confluence was reached. Next, a single wound was created in the monolayer cells by gently scratching the attached cells with a sterile 10 μl micropipette tip (time 0 h). After scratching, the cells were incubated with serum-free DMEM medium for 24 h. Cell migration was photographed using fluorescence microscopy (IX70; Olympus, Japan) and ax10 objective at 48 h following injury. Remodeling was measured as the diminishing distance across the induced injury, normalized to the 0 h control, and expressed as relative migration. Each experiment was performed at least three times independently.

Western blot analysis. Protein was extracted from tissues using radioimmunoprecipitation assay (RIPA buffer) (BeyotimeInstitute of Biotechnology, Shanghai, China) buffer containing a 1/10 Complete Miniprotease inhibitor cocktail (Roche Diagnostics GmbH, Mannheim, Germany). RIPA lysate was added into the samples, at 0˚C for 30 min following vortex blending, and then a 10 min intermittent oscillation was performed. The protein concentration

Table I. Primers used in RT-qPCR.

Primer	Sequence (5'-3')	No. of bases
ZNF689-forward	TGGAACGAAACACCGATGACT	21
ZNF689-reverse	CCATTCTTCTTTCTGGTTCTGCT	23
GAPDH-forward	ACTCCTCCACCTTTGACGC	19
GAPDH-reverse	GCTGTAGCCAAATTCGTTGTC	21

ZNF, zinc finger protein.

was measured using a bicinchoninic acid protein assay kit (Beyotime, Institute of Biotechnology). Following denaturing at 95˚C for 10 min, 50 μg of each protein sample was separated using SDS-PAGE (10% gel) and then transferred to a polyvinylidene difluoride membrane. Subsequent to blocking with 5% nonfat dry milk in TBS with 0.1% Tween-20 (TBST) for 1 h at room temperature, the membrane was incubated with primary antibodies at 4˚C overnight. The primary antibodies used for western blot included ZNF-689 from Sigma-Aldrich, Merck KGaA, Darmstadt, Germany (1:1,000, Cat no. SAB1408243), E-cadherin (1:1,000, Cat no. 3195T), β-catenin (1:1,000, Cat no. 8480T) and Snail 1 (1:1,000, Cat no. 3879T) from Cell signaling Technology, Inc., Danvers, MA, USA, the GAPDH employed as normalized control from Zen BioScience (1:2,000, Cat no. 220068, Chengdu, China). Subsequent to washing three times with TBST buffer for 10 min per wash, the membrane was further incubated at room temperature for 1 h with horseradish peroxidase conjugated rabbit anti-mouse IgG (cat no. 250097) or mouse anti-rabbit (cat no. 701051) Secondary antibodies were also purchased from Zen BioScience, (Chengdu, China) and used at a dilution of 1:5,000. Subsequently, the results were scanned with a Chemical Mp Imaging System (Bio-Rad Laboratories). Following treatment with immobilon ECL ultra western HRP substrate of Millipore (Merck KGaA, Darmstadt, Germany) according to the manufacturer's protocol the expression levels of each protein was quantified by Image J software version 1.8.0 (National Institutes of Health, Bethesda, MD, USA).

Immunohistochemistry (IHC) staining. IHC was conducted according to the instructions of the SP-9001 kit (Beyotime Institute of Biotechnology). Images were observed at magnification, x400 under a fluorescence microscope. 10% formalin-fixed, paraffin-embedded tissue sections of representative areas of tumor were cut into 4 μm-thick sections. IHC was performed with a standard two-step method. First, the slides were de-paraffinized with xylene and rehydrated a graded alcohol series (100, 90, 70 and 50% ethyl alcohol) for 10 min at room temperature, and antigen retrieval was performed by incubating samples in sodium citrate buffer (pH 6.0) for 30 min at 98˚C. Inactivation of endogenous peroxidase was performed with a 3% hydrogen peroxide solution for 20 min at room temperature. After 30 min blocking (5% normal goat serum purchased from Beyotime Institute of Biotechnology) at room temperature), the tissue sections were incubated with rabbit polyclonal anti-ZNF689 primary antibodies (SAB2701570; dilution 1:100) (Sigma-Aldrich; Merck KGaA) overnight at 4˚C. Subsequent to washing, the slides were incubated with horseradish peroxidase-conjugated secondary antibody for 40 min at 37˚C (SAB2701462; dilution 1:500) (Sigma-Aldrich; Merck KGaA).

IHC staining was evaluated by an immunoreactivity score (IRS), which was calculated by multiplying the staining intensity and extent as previously described (17). Deng DW who works in Department of hepato-biliary-pancrease of Affiliated Hospital of North Sichuan College performed IHC and he was blinded to the mRNA ZNF689 expression results. The staining intensity was classified as: 0(negative), 1(weak), 2(moderate) or 3(strong). Based on the percentage of positively stained cells throughout the tumor, the extent of staining was defined as 0(0%), 1(<10%), 2(10%-50%), 3(51%-80%) or 4(>80%). IRS score is the staining intensity score multiplied by the extent of staining score, ranging from 0 to 12, with an IRS score of ≥4 defined as positive expression, and an IRS score of <4 defined as negative expression.

Statistical analysis. Statistical analysis was performed using SPSS software (version 21.0; IBM Corp, Armonk, NY, USA) and GraphPad Prism software (version 5.00; GraphPad Software, Inc., La Jolla, CA, USA). $P<0.05$ was considered to indicatea statistically significant difference. Continuous variables are presented as the mean ± standard deviation or mean ± standard difference with 95% confidence intervals (CI). An unpaired Student's t-tests or one-way analysis of variance tests were performed to compare continuous variables with parametric distributions, the post-hoc test used following the analysis of variance was Student Newman Keuls test. Categorical data were analyzed using the chi-squared or Fisher's exact tests. Survival data were calculated with the Kaplan-Meier method and compared by the log-rank test. Univariate and multivariate analyses were performed using Cox's regression method.

Results

Expression of ZNF689 in HCC, paired non-cancerous tissue, and normal liver tissue. RT-qPCR analysis revealed no significant difference in the expression of ZNF689 mRNA between HCC and paired non-cancerous tissues, with a mean difference of -0.26 (95% CI, -1.32, 0.80; P=0.62). In addition, the expression of ZNF689 mRNA was detected in 16 normal liver tissues collected from patients with hemangioma who underwent liver resection in West China Hospital of Sichuan University from January 2011 to December 2012. The diagnosis of hemangioma

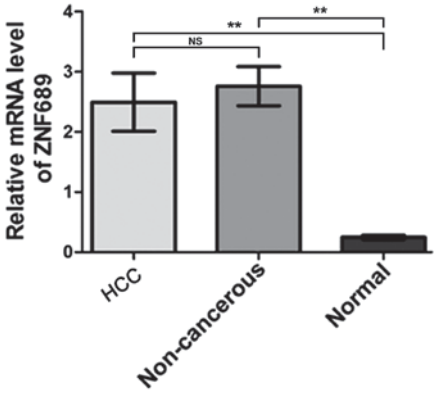

Figure 1. Relative mRNA levels of ZNF689 in hepatocellular carcinoma tissues, paired non-cancerous tissues, and normal tissues. ZNF, zinc finger protein. **P<0.05.

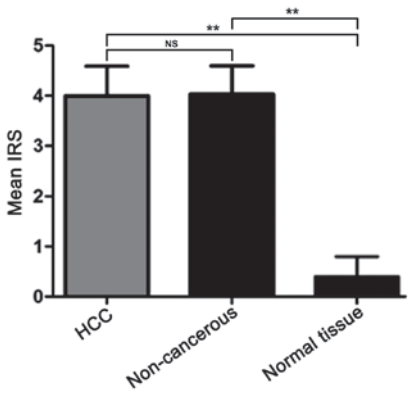

Figure 2. Comparison of zinc finger protein 689 protein expression in HCC tissues, paired non-cancerous tissues, and normal tissues. HCC, hepatocellular carcinoma; IRS, immunoreactivity score. **P<0.05.

was based on pathological test, and patients with hemangioma who have not received any systematic or local therapy were included, those who also complicated with tumor lesions in other organs were excluded. Of these 16 patients, 10 were female, 6 were male, and the median age was 41.7 years (age range 27-68 years). All these 16 patients were diagnosed as hemangioma and not included in the above 102 patients. The results demonstrated that ZNF689 mRNA expression was increased in HCC tissues and paired non-cancerous tissues compared with the normal liver tissues. The differences between means were 2.246±0.4840 (95% CI, 1.278, 3.214) and 2.510±0.3273 (95% CI, 1.856, 3.165), respectively (P<0.05; Fig. 1).

IHC analysis demonstrated that the mean IRS score was 4, 4.03, and 0.4 in the tumor, paired non-cancerous and normal liver tissues, respectively (Fig. 2). IHC revealed positive expression of ZNF689 protein (IRS score ≥4) in 45 cases (45/102, 44.12%) of HCC and 45 cases (45/102, 44.12%) of paired non-cancerous tissues. There was no significant difference in the expression levels of the ZNF689 protein between HCC and paired non-cancerous tissues, and the mean difference of the ZNF689 protein in HCC and non-cancerous tissues was -0.02941 (95% CI, -1.587, 1.528, P=0.97). However, the expression levels of the ZNF689 protein in HCC and non-cancerous tissues were significantly higher compared with those in normal liver tissues (P<0.05; Fig. 2). Representative images of the IHC analysis are presented in Fig. 3.

The relative mRNA levels of ZNF689 were analyzed in the positive and the negative expression group and it was identified that the mRNA level in the positive expression group was significantly increased compared with that in the negative expression group (P=0.038), indicating that ZNF689 expression was consistent between them RNA and protein level (Fig. 4).

Association between ZNF689 levels in HCC tissues and clinicopathological parameters. Associations between ZNF689 expression in HCC and clinicopathological parameters is summarized in Table II. Positive expression of the ZNF689 protein in HCC was significantly associated with a tumor size of ≥10 cm (P=0.028), tumor capsule infiltration (P=0.005) and microvascular invasion (MVI; P=0.037). No significant association was observed between expression of the ZNF689 protein and age, sex, HBV surface antigen, the extent of cirrhosis, tumor number, portal vein embolus, BCLC stage or differentiation.

Positive expression of ZNF689 in HCC is associated with poor prognosis. Follow-up was completed in May 2016. Since the majority of the patients enrolled in the present study were from a rural area in China, a lack of compliance with treatment guidelines and financial difficulties resulted in a relatively high incidence of loss to follow-up.

Of the 63 patients who completed the follow-up, 47 (74.6%) experienced recurrence and 39 (61.9%) patients had succumbed to the disease by the follow-updeadline. The median follow-up time was 33 months (range, 1-65 months). The overall survival (OS) rate was 38.1% (24/63), with a median OS of 33 months. The median progression-free survival (PFS) was 20 months.

Patients with follow-up data were grouped into two categories according to the IRS in HCC tissues. The median OS in the positive expression group (27±1.10 months; 95% CI, 24.85-29.15) was significantly lower compared with that in the negative expression group (47±6.33 months; 95% CI, 34.59-59.41; χ^2=3.954; P=0.047; Fig. 5). The median PFS in the positive expression group (19±1.40 months; 95% CI, 15.28-20.73) was also significantly lower compared with that in the negative expression group (23±4.17; 95% CI, 14.85-31.16; χ^2=4.762; P=0.029; Fig. 6).

Prognostic factors for OS and PFS. Univariate analysis indicated that cancer embolus in the portal vein [hazard ratio (HR), 3.894; P=0.013], MVI (HR, 3.109; P=0.040) and positive expression of ZNF689 (HR, 2.033; P=0.041) were prognostic factors for OS. Multiple tumors (HR, 2.399; P=0.019), cancer embolus in the portal vein (HR, 2.388; P=0.009), tumor capsule infiltration (HR, 2.398; P=0.013), MVI (HR, 2.799; P=0.002) and positive expression of ZNF689 (HR, 1.967; P=0.036) were prognostic factors for PFS detected by univariate analysis.

For multivariate analysis, the known prognostic factors by univariate analysis were selected together with the known significant clinical variables. Cancer embolus in the portal vein (HR, 2.298; P=0.038), MVI (HR, 2.178; P=0.047) and positive expression of ZNF689 (HR, 1.961; P=0.048) were significantly associated with OS, whereas multiple tumors (HR, 1.398; P=0.021), cancer embolus in the portal vein (HR,

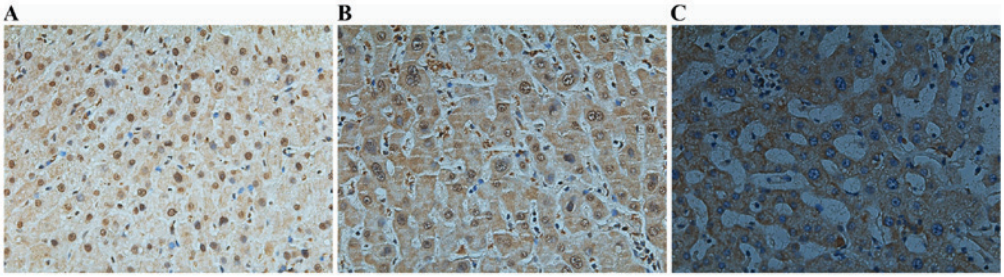

Figure 3. Representative immunohistochemical images of zinc finger protein 689 stainingin HCC, non-cancerous tissues, and normal tissues. (A) HCC tissue. (B) Paired non-cancerous tissue. (C) Normal liver tissue. Magnification, x400. HCC, hepatocellular carcinoma.

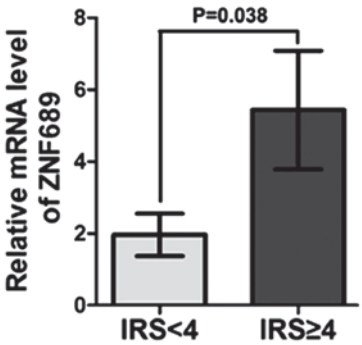

Figure 4. Relative mRNA level of ZNF689 in the positive and negative expression groups. ZNF, zinc finger protein; IRS, immunoreactivity score.

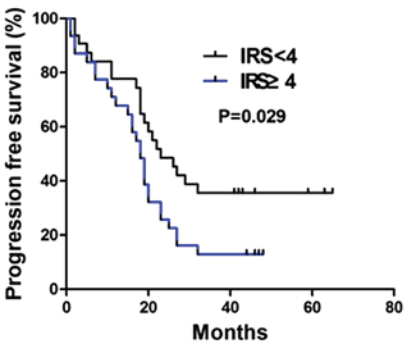

Figure 6. Association between zinc finger protein 689 expression in hepatocellular carcinoma and progression-free survival. IRS, immunoreactivity score.

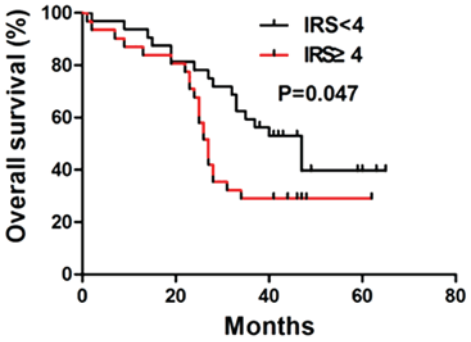

Figure 5. Association between zinc finger protein 689 expression in hepatocellular carcinoma and overall survival. IRS, immunoreactivity score.

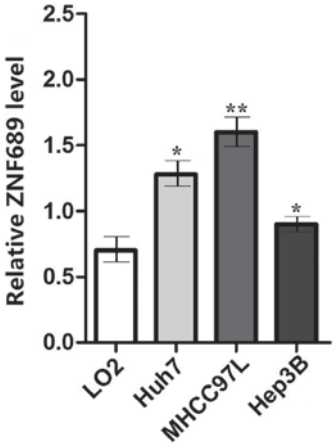

Figure 7. Comparison of ZNF689 expression in LO2 and hepatocellular carcinoma cell lines. *P<0.05 and **P<0.01 vs. LO2 cells. ZNF, zinc finger protein.

1.561; P=0.045), MVI (HR, 2.108; P=0.014) and positive expression of ZNF689 (HR, 1.902; P=0.041) were prognostic factors for PFS (Table III).

Underlying mechanism of ZNF689 regulating invasion and migration of HCC. The ZNF689 expression was evaluated in LO2 cells and three HCC cell lines (Huh7, MHCC97H and Hep3B). It was identified that the expression of ZNF689 in HCC cell lines was significantly higher compared with that in LO2 (P<0.05; Fig. 7). ZNF689 was knocked down and over-expressed in the HCC cell line MHCC97L, and it was revealed that knockdown of ZNF689 substantially suppressed the proliferation and migration of HCC cells (Fig. 8).

To investigate the potential underlying molecular mechanism of ZNF689 regulating the invasion and migration of HCC, the expression of E-cadherin, which is the most important biomarker of the epithelial-mesenchymal transition (EMT), was investigated in normal and ZNF689 knockdown MHCC97L cells. The expression of E-cadherin was higher in ZN689 knockdown MHCC97L cells compared with that in normal MHCC97L cells (Fig. 9), which revealed the potential role of ZNF689 in regulating the EMT process. Further supporting the function of ZNF689 in regulating EMT, the expression of β-catenin and the target gene SNAIL1 were substantially decreased following knockdown of ZNF689 in MHCC97L cells, SNAIL1 is the abbreviation of snail family transcriptional repressor 1, which is a member of transcription factors, is critical for inducing and sustaining cancer EMT (18) (Fig. 10). It is hypothesized that ZNF689 may regulate the EMT of HCC via the Wnt-β-catenin-snail signaling pathway.

Table II. Associations between ZNF689 expression levels and the clinical characteristics of patients with hepatocellular carcinoma.

Characteristics	Positive expression (IRS score ≥4)	Negative expression (IRS score <4)	P-value
Sex			0.495
Male	42	51	
Female	3	6	
Age (years)			0.171
>60	12	30	
<60	33	27	
α-fetoprotein (ng/ml)			0.549
>400	24	27	
<400	21	30	
Hepatitis B surface antigen			0.492
Positive	45	51	
Negative	0	6	
HBV-DNA			0.495
$>10^3$/copies	30	30	
$<10^3$/copies	15	27	
Child-Pugh classification			0.764
Child A	42	54	
Child B	3	3	
Liver cirrhosis			0.506
Yes	33	45	
No	12	12	
Tumor number			0.613
Single	42	48	
Multiple	3	9	
Tumor size (cm)			0.028
>10	18	3	
<10	27	54	
Tumor size (cm)			0.104
>5	42	39	
<5	3	18	
Cancer embolus in portal vein			0.718
Yes	15	15	
No	30	42	
BCLC stage			0.410
BCLC A	3	12	
BCLC B	21	27	
BCLC C	21	18	
Tumor capsule			0.005
Complete infiltration	6	36	
No capsule infiltration	39	21	
Microvascular invasion			0.037
Yes	33	18	
No	12	39	
Differentiation			0.273
High	3	3	
Moderate	42	45	
Low	0	9	

BCLC, Barcelona clinic liver cancer staging; HBV, hepatitis B virus.

Discussion

The aim of the present study was to investigate the expression of ZNF689 in HCC at the mRNA and protein expression levels. Its expression did not differ significantly between HCC tissues and paired non-cancerous tissues. However, the expression of ZNF689 in HCC tissues and paired non-cancerous tissues was significantly higher compared with that in normal liver tissues. Positive expression of ZNF689 was significantly associated with a tumor size >10 cm, MVI and tumor capsule infiltration. Additionally, the positive expression of ZNF689 in HCC was associated with the poor prognosis of HCC.

ZNF689 has previously been implicated in the development of HCC. Silva *et al* (8) analyzed the gene-expression profiles of 20 HCC tissue samples, and identified a novel gene (transcription-involved protein upregulated in HCC) that encoded a 500-amino-acid protein containing 12 zinc-finger domains and a Kruppel-associated box domain, which was later termed ZNF689. ZNF689 was identified to be involved in suppressing the apoptosis of HCC cells via downregulation of the expression of pro-apoptotic factors.

ZNF689 protein expression was detected by IHC in 102 cases of HCC tissues and paired non-cancerous tissues in the present study and 45 of the HCC cases were positive for expression of ZNF689, which was consistent with previous results (13), including a study by Shigematsu *et al* (13), reporting that ZNF689 knockdown induced expression of the pro-apoptotic factors of the Bcl-2 family, Bax, Bcl-2 antagonist/killer 1 and Bid, resulting in tumor cell apoptosis. Suppression of tumor cell apoptosis by ZNF689 is reflected by increased tumor burden, as indicated by tumor size. Hu *et al* (19) demonstrated that Bcl-2 associated death promoter (Bad) serves a key function in HCC development, and that low expression of Bad is associated with larger tumor size and poor prognosis. It was also identified that HCC tumor cell growth was inhibited by microRNA-204 via downregulation of Bcl-2, and low expression of microRNA-204 is markedly associated with increased tumor size (20). These data are consistent with the results of the present study, indicating an association between HCC cell apoptosis and solid tumor size.

Table III. Prognostic factors for overall survival and progression-free survival by univariate and multivariate analysis.

A, Univariate analysis

Factors	Overall survival			Progression free survival		
	HR	95% CI	P-value	HR	95% CI	P-value
Age (years, >60 vs. <60)	0.458	(0.156,1.348)	0.156	1.246	(0.700,2.219)	0.455
α-fetoprotein (ng/ml, >400 vs. <400)	0.774	(0.280,2.138)	0.621	0.956	(0.518,1.764)	0.886
Hepatitis B surface antigen (positive vs. negative)	0.653	(0.085,5.015)	0.682	2.402	(0.329,17.528)	0.387
HBV-DNA (copies, $>10^3$ vs. $<10^3$)	0.613	(0.217,1.730)	0.355	0.810	(0.441,1.488)	0.497
Child-Pugh classification (Child B vs. Child A)	2.466	(0.317,19.198)	0.389	1.451	(0.349,6.039)	0.609
Liver cirrhosis (Yes vs. no)	1.989	(0.440,8.989)	0.372	1.639	(0.725,3.704)	0.235
Tumor number (multiple vs. single)	1.681	(0.465,6.081)	0.428	2.399	(1.153,4.989)	0.019
Tumor size (cm, >10 vs. <10)	1.291	(0.569,2.930)	0.541	1.405	(0.655,3.015)	0.383
Tumor size (cm, >5 vs. <5)	0.899	(0.300,2.696)	0.850	1.432	(0.715,2.869)	0.311
Cancer embolus in portal vein (Yes vs. no)	3.849	(1.331,11.126)	0.013	2.388	(1.238,4.605)	0.009
Tumor capsule (infiltration vs. complete)	1.579	(0.537,4.643)	0.406	2.398	(1.201,4.788)	0.013
Microvascular invasion (Yes vs. no)	3.109	(1.108,9.976)	0.040	2.799	(1.464,5.351)	0.002
Differentiation High+moderate vs. low	1.313	(0.455,3.792)	0.615	1.155	(0.616,2.169)	0.653
ZNF689 expression (positive vs. negative)	2.033	(1.054,3.920)	0.041	1.967	(1.092,3.543)	0.036

B, Multivariate analysis

Factors	Overall survival			Progression free survival		
	HR	95% CI	P-value	HR	95% CI	P-value
Tumor number (multiple vs. single)	1.473	(0.116,1.929)	0.297	1.398	(1.181,2.872)	0.021
Cancer embolus in portal vein (Yes vs. no)	2.298	(1.481,4.835)	0.038	1.561	(1.058,3.922)	0.045
Tumor capsule (infiltration vs. complete)	0.946	(0.294,3.014)	0.926	1.597	(0.750,3.401)	0.225
Microvascular invasion (Yes vs. no)	2.178	(1.118,4.245)	0.047	2.108	(1.162,3.825)	0.014
ZNF689 expression (positive vs. negative)	1.961	(1.023,3.758)	0.048	1.902	(1.061,3.412)	0.041

HR, hazard ration; CI, confidence interval; ZNF, zinc finger protein; HBV, hepatitis B virus.

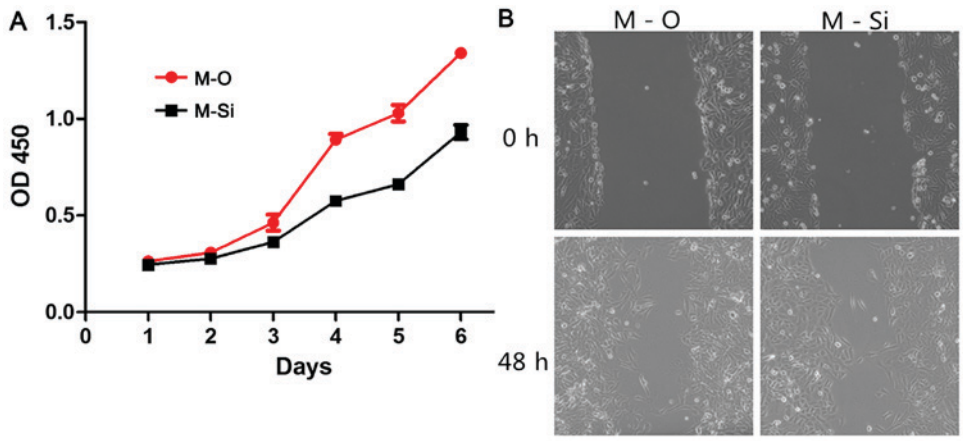

Figure 8. Comparison of proliferation and migration between ZNF689 M-Si and M-O cell lines. (A) Proliferation experiment. (B) Migration experiment. M-Si, ZNF689 knockdown; M-O, ZNF689 overexpression; znf, zinc finger protein; OD, optical density.

MVI is an important indicator of poor prognosis for patients receiving radical liver resection; patients without MVI have improved short- and long-term survival outcomes and a lack of MVI is associated with short- and long-term

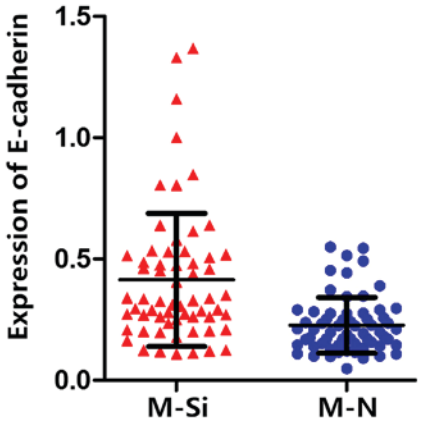

Figure 9. Expression of E-cadherin in zinc finger protein 689 M-Si and M-NMHCC97L cells. M-Si, knockdown; M-N, normal.

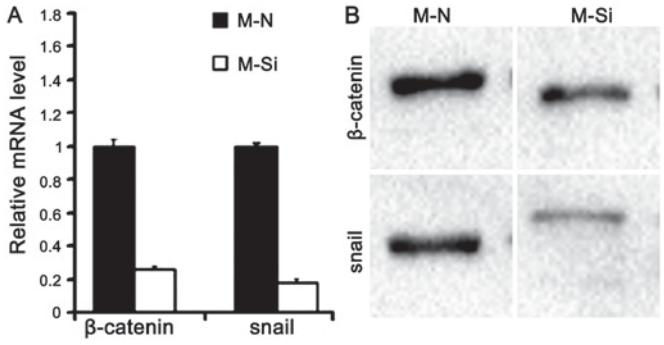

Figure 10. Knockdown of zinc finger protein 689 resulted in the downregulation of β-catenin and snail. (A) Result of reverse transcription-quantitative polymerase chain reaction. (B) Result of western blotting.

recurrence rate (21). Previous studies have revealed that tumor size is a predictor of MVI (22-24). For example, a cohort of patients from Australia was retrospectively analyzed, and investigators identified that a tumor size >5 cm was independently associated with MVI (25). Since positive expression of ZNF689 was associated with larger tumor size, it may also be directly associated with the presence of MVI. Although a variety of studies have investigated the association between tumor angiogenesis and MVI, the mechanism of MVI has not yet been completely elucidated. The question of whether ZNF689 serves a key function in the angiogenesis of HCC requires further investigation.

The tumor capsule is a unique characteristic of HCC, functioning as a barrier preventing cancer cell invasion of adjacent tissues or distant organs (26). Investigators have reached a consensus that tumor capsule infiltration is an important prognostic factor of HCC following liver resection. Iguchi *et al* (26) suggested that extracapsular penetration is a prognostic factor of overall and disease-free survival, and demonstrated that the percentage of tumor capsule infiltration in larger tumor types is increased compared with that in smaller tumor types (27). Consequently, tumor capsule infiltration may be considered as a result of tumor cell growth (28). Consistent with these results, ZNF689 was identified to participate in suppressing the apoptosis of HCC tumor cells, and inhibition of cell apoptosis may increase the diameter of solid tumor types, which may also lead to tumor capsule infiltration.

Considering the mechanism of ZNF689 in regulating the invasive ability of HCC, a series of *in vitro* experiments were performed. ZNF689 knockdown and overexpressed HCC cell lines were established and the expression of biomarkers and important components of EMT were compared. The present study demonstrated that the knockdown of ZNF689 may inhibit proliferation and invasion of HCC cells by the Wnt-β-catenin-snail pathway. It is known that EMT is associated with the progressive ability of numerous malignant tumors (29). Currently, three signaling pathways have been demonstrated to regulate the EMT process (30,31). The wnt-β-catenin signaling pathway has been demonstrated to serve key functions in regulating HCC invasion and migration by previous studies. Snail is a common target gene in the wnt-β-catenin pathway, which serves critical functions at the post-transcriptional level (32). The present study identified the association between ZNF689 alteration and the wnt-β-catenin pathway, however, *in vivo* experiments should be performed for further confirmation.

The present study had several limitations. First, a comparatively high rate of loss to follow-up reduced the reliability of the survival analysis. Furthermore, the majority of the patients in the present study suffered from a HBV infection, with underlying liver cirrhosis. Whether a difference in ZNF689 expression between HCC tissue and normal liver tissue also exists in non-cirrhotic HCC requires further investigation.

In conclusion, the present study demonstrated that ZNF689 was upregulated in HCC tissues compared with normal liver tissues, and the expression level of ZNF689 was associated with tumor size, MVI and tumor capsule infiltration. Positive expression of ZNF689 was identified to be a poor prognostic factor for OS and progression-free survival. These data suggest that ZNF689 may be a novel factor in the design of treatment strategies for HCC and in predicting the prognosis of patients with HCC following liver resection. Inhibitors of ZNF689 may be designed to knockdown expression of ZN689 and serve as a complementary strategy to HCC treatment.

Acknowledgements

The authors would like to acknowledge the support of the Department of Pathology and Clinical Sample Bank of West China Hospital.

Funding

The present study was funded by grants from the National Natural Science Foundation of China (grant. no. 71673193), and the Key Technology Research and Development Program of the Sichuan Province (grant. no. 2015SZ0131).

Availability of data and materials

All data generated or analyzed during this study are included in this published article.

Authors' contributions

PY wrote the paper and undertook the majority of experiments, BW and GZ were responsible for data collection, DD analyzed the available data, JL proposed the idea and approved the submission of the present study.

Ethics approval and consent to participate

Written informed consent was obtained from all enrolled patients, and the study was ethically approved by the Biomedical Ethics Committee of West China Hospital.

Patient consent for publication

Written informed consent was obtained from all study participants for publication associated data and images in this study.

Competing interests

The authors declare that they have no competing interests.

References

1. Mazzanti R, Arena U and Tassi R: Hepatocellular carcinoma: Where are we? World J Exp Med 6: 21-36, 2016.
2. Bruix J, Reig M and Sherman M: Evidence-based diagnosis, staging, and treatment of patients with hepatocellular carcinoma. Gastroenterology 150: 835-853, 2016.
3. Yi PS, Zhang M and Xu MQ: Management of the middle hepatic vein in right lobe living donor liver transplantation: A meta-analysis. J Huazhong Univ Sci Technolog Med Sci 35: 600-605, 2015.
4. Llovet JM, Bru C and Bruix J: Prognosis of hepatocellular carcinoma: The BCLC staging classification. Semin Liver Dis 19: 329-338, 1999.
5. Llovet JM, Ricci S, Mazzaferro V, Hilgard P, Gane E, Blanc JF, de Oliveira AC, Santoro A, Raoul JL, Forner A, *et al*: Sorafenib in advanced hepatocellular carcinoma. N Engl J Med 359: 378-390, 2008.
6. Hu MD, Jia LH, Liu HB, Zhang KH and Guo GH: Sorafenib in combination with transarterial chemoembolization for hepatocellular carcinoma: A meta-analysis. Eur Rev Med Pharmacol Sci 20: 64-74, 2016.
7. Yuan SX, Yang F, Yang Y, Tao QF, Zhang J, Huang G, Yang Y, Wang RY, Yang S, Huo XS, *et al*: Long noncoding RNA associated with microvascular invasion in hepatocellular carcinoma promotes angiogenesis and serves as a predictor for hepatocellular carcinoma patients' poor recurrence-free survival after hepatectomy. Hepatology 56: 2231-2241, 2012.
8. Silva FP, Hamamoto R, Furukawa Y and Nakamura Y: TIPUH1 encodes a novel KRAB zinc-finger protein highly expressed in human hepatocellular carcinomas. Oncogene 25: 5063-5070, 2006.
9. Wang Q, Tan YX, Ren YB, Dong LW, Xie ZF, Tang L, Cao D, Zhang WP, Hu HP and Wang HY: Zinc finger protein ZBTB20 expression is increased in hepatocellular carcinoma and associated with poor prognosis. BMC Cancer 11: 271, 2011.
10. Kan H, Huang Y, Li X, Liu D, Chen J and Shu M: Zinc finger protein ZBTB20 is an independent prognostic marker and promotes tumor growth of human hepatocellular carcinoma by repressing FoxO1. Oncotarget 7: 14336-14349, 2016.
11. Yang Z, Sun B, Li Y, Zhao X, Zhao X, Gu Q, An J, Dong X, Liu F and Wang Y: ZEB2 promotes vasculogenic mimicry by TGF-β1 induced epithelial-to-mesenchymal transition in hepatocellular carcinoma. Exp Mol Pathol 98: 352-359, 2015.
12. Wu D, Liu G, Liu Y, Saiyin H, Wang C, Wei Z, Zen W, Liu D, Chen Q, Zhao Z, *et al*: Zinc finger protein 191 inhibits hepatocellular carcinoma metastasis through discs large 1-mediated yes-associated protein inactivation. Hepatology 64: 1148-1162, 2016.
13. Shigematsu S, Fukuda S, Nakayama H, Inoue H, Hiasa Y, Onji M and Higashiyama S: ZNF689 suppresses apoptosis of hepatocellular carcinoma cells through the down-regulation of Bcl-2 family members. Exp Cell Res 317: 1851-1859, 2011.
14. Jiang BG, Wan ZH, Huang J, Li LM, Liu H, Fu SY, Yang Y, Zhang J, Yuan SX, Wang RY, *et al*: Elevated ZC3H15 increases HCC growth and predicts poor survival after surgical resection. Oncotarget 7: 37238-37249, 2016.
15. Papatheodoridis GV, Cholongitas E, Dimitriadou E, Touloumi G, Sevastianos V and Archimandritis AJ: MELD vs Child-Pugh and creatinine-modified Child-Pugh score for predicting survival in patients with decompensated cirrhosis. World J Gastroenterol 11: 3099-3104, 2005.
16. Livak KJ and Schmittgen TD: Analysis of relative gene expression data using real-time quantitative PCR and the 2(-Delta Delta C(T)) method. Methods 25: 402-408, 2001.
17. Specht E, Kaemmerer D, Sanger J, Wirtz RM, Schulz S and Lupp A: Comparison of immunoreactive score, HER2/neu score and H score for the immunohistochemical evaluation of somatostatin receptors in bronchopulmonary neuroendocrine neoplasms. Histopathology 67: 368-377, 2015.
18. Xu W, Liu H, Liu ZG, Wang HS, Zhang F, Wang H, Zhang J, Chen JJ, Huang HJ, Tan Y, *et al*: Histone deacetylase inhibitors upregulate Snail via Smad2/3 phosphorylation and stabilization of Snail to promote metastasis of hepatoma cells. Cancer Lett 420: 1-13, 2018.
19. Hu W, Fu J, Lu SX, Liu LL, Luo RZ, Yun JP and Zhang CZ: Decrease of Bcl-xL/Bcl-2-associated death promoter in hepatocellular carcinoma indicates poor prognosis. Am J Cancer Res 5: 1805-1813, 2015.
20. Li K, Xyu Q, Liu X, Liu Q and Wang M: Growth inhibition of human hepatocellular carcinoma by miRNA-204 via down-regulation of Bcl-2 and Sirt1 expression. Xi Bao Yu Fen Zi Mian Yi Xue Za Zhi 31: 168-172, 2015 (In Chinese).
21. Yu YQ, Wang L, Jin Y, Zhou JL, Geng YH, Jin X, Zhang XX, Yang JJ, Qian CM, Zhou DE, *et al*: Identification of serologic biomarkers for predicting microvascular invasion in hepatocellular carcinoma. Oncotarget 7: 16362-16371, 2016.
22. Shen J, Wen J, Li C, Wen T, Yan L, Li B, Yang J and Lu C: The prognostic value of microvascular invasion in early-intermediate stage hepatocelluar carcinoma: A propensity score matching analysis. BMC Cancer 18: 278, 2018.
23. Giannini EG, Bucci L, Garuti F, Brunacci M, Lenzi B, Valente M, Caturelli E, Cabibbo G, Piscaglia F, Virdone R, *et al*: Patients with advanced hepatocellular carcinoma need a personalized management: A lesson from clinical practice. Hepatology 67: 1784-1796, 2018.
24. Imai K, Yamashita YI, Yusa T, Nakao Y, Itoyama R, Nakagawa S, Okabe H, Chikamoto A, Ishiko T and Baba H: Microvascular invasion in small-sized hepatocellular carcinoma: Significance for outcomes following hepatectomy and radiofrequency ablation. Anticancer Res 38: 1053-1060, 2018.
25. Schlichtemeier SM, Pang TC, Williams NE, Gill AJ, Smith RC, Samra JS, Lam VW, Hollands M, Richardson AJ, Pleass HC, *et al*: A pre-operative clinical model to predict microvascular invasion and long-term outcome after resection of hepatocellular cancer: The Australian experience. Eur J Surg Oncol 42: 1576-1583, 2016.
26. Iguchi T, Aishima S, Taketomi A, Nishihara Y, Fujita N, Sanefuji K, Maehara Y and Tsuneyoshi M: Extracapsular penetration is a new prognostic factor in human hepatocellular carcinoma. Am J Surg Pathol 32: 1675-1682, 2008.
27. Iguchi T, Aishima S, Sanefuji K, Fujita N, Sugimachi K, Gion T, Taketomi A, Shirabe K, Maehara Y and Tsuneyoshi M: Both fibrous capsule formation and extracapsular penetration are powerful predictors of poor survival in human hepatocellular carcinoma: A histological assessment of 365 patients in Japan. Ann Surg Oncol 16: 2539-2546, 2009.
28. Li Y, Xu D, Bao C, Zhang Y, Chen D, Zhao F, Ding J, Liang L, Wang Q, Liu L, *et al*: MicroRNA-135b, a HSF1 target, promotes tumor invasion and metastasis by regulating RECK and EVI5 in hepatocellular carcinoma. Oncotarget 6: 2421-2433, 2015.
29. Brabletz T: Metastasis: EMT, microRNAs and cancer stem cells. Clin Experimental Metastasis 32: 187-187, 2015.
30. Lamouille S, Xu J and Derynck R: Molecular mechanisms of epithelial-mesenchymal transition. Nat Rev Mol Cell Biol 15: 178-196, 2014.
31. Kalluri R and Weinberg RA: The basics of epithelial-mesenchymal transition. J Clin Invest 119: 1420-1428, 2009.
32. Yang JD, Nakamura I and Roberts LR: The tumor microenvironment in hepatocellular carcinoma: Current status and therapeutic targets. Semin Cancer Biol 21: 35-43, 2011.

This work is licensed under a Creative Commons Attribution-NonCommercial-NoDerivatives 4.0 International (CC BY-NC-ND 4.0) License.